DESIGN OF A PULSED CRYOMAGNET GENERATING 5T PEAK MAGNETIC FLUX DENSITY

I. DOBRIN[1], D. ENACHE[2], G. DUMITRU[3], A. DOBRIN[4], R. PINTEA[5], S. ZAMFIR[6]

In this paper, are presented a conceptual model and the design of a conventional electromagnet, made in a Helmholtz arrangement of the copper coils. The magnet is cooled to the temperature of liquid nitrogen (77 K) to obtain an intense magnetic field, with field magnetic flux density of maximum 5T and high uniformity (1-3%) in the central area of the coils. The numerical modeling made in Comsol Multiphysics allowed the optimization of the electromagnet, to obtain the magnetic flux density of 5T, with the adequate geometry and a minimum material consumption. Powered in pulsating regime, the electromagnet winding is periodically subjected to heating and cooling, thermal process is also evaluated to optimize the electromagnet functionality and to obtain the projected parameters at the preset values.

Keywords: electromagnet, magnetic field, cryogenics, numerical simulations

1. Introduction

Discovery of both new superconducting materials with "high" critical temperature (HTS-high temperature superconductors) [1,2] and the improvement of technologies for obtaining the existing ones (LTS - Low temperature Superconductors) [3,4,5], increased the performance of various types of electromagnets used for particle accelerators. As a consequence, they contributed to the obtaining of new electromagnets for higher acceleration energies of particles which give rise for new discoveries in physics [6]. Also, new applications were developed for high-speed transport (magnetic levitation trains)

[1] Scientific researcher, National Institute for R&D in Electrical Engineering ICPE-CA, Bucharest, România, e-mail: ion.dobrin@icpe-ca.ro
[2] Scientific researcher, National Institute for R&D in Electrical Engineering ICPE-CA, Bucharest, România, e-mail: dan.enache@icpe-ca.ro
[3] Scientific researcher, National Institute for R&D in Electrical Engineering ICPE-CA, Bucharest, România, e-mail: george.dumitru@icpe-ca.ro
[4] Scientific researcher, National Institute for R&D in Electrical Engineering ICPE-CA, Bucharest, România, e-mail: andrei.dobrin@icpe-ca.ro
[5] Scientific researcher, National Institute for R&D in Electrical Engineering ICPE-CA, Bucharest, România, e-mail: radu.pintea@icpe-ca.ro
[6] Scientific researcher, National Institute for R&D in Electrical Engineering ICPE-CA, Bucharest, România, e-mail: stefania.zamfir@icpe-ca.ro

[7], applications in electrical engineering (motors, generators, electricity transmission lines, transformers, superconducting current limiters, etc.) [8, 9,10]. These applications have much higher performances than the conventional ones and most important, without losses. Medicine has also benefited from the improvement of imaging methods for investigating the human body (MRI or superconducting computed tomography) and ultramodern treatment systems for various types of tumors located in sensitive areas of the body (brain, internal organs etc.), through the so-called hadron therapy [11]. Hadron therapy requires the use of an accelerated and very well focused flux of particles / ions, so of some electromagnets, both for the control of the accelerated beam direction and for the transverse focusing of the beam. This rigorous control requires the use of dipole superconducting electromagnets [12, 13] as well as quadripolar electromagnets [14]. The same type of electromagnets are used in modern accelerators for the same purpose. Thus, the realization of these types of superconducting electromagnets, including solenoid type [15], are crucial for these top applications of superconductors. However, their realization also requires the use of cryogenics to obtain and maintain the thermal regime of operation for superconductors: 4.2 - 77K. LTS superconductors require the use of liquid helium (4.2K) but HTS superconductors can also be used at liquid nitrogen temperature (77K). Advances in this field have led to the development of devices called closed-cycle cryocoolers of McMahon [16] type or "pulse-tube" type [17, 18], which have made it possible to obtain cryogenic temperatures without cryogenic agents, namely by conductive cooling. In this sense, the cryocooler works as a heat pump, taking the body heat to be cooled and evacuating it out of the system.

2. Cryomagnet design

2.1. Conceptual model of cryomagnet

The conceptual model of the cryomagnet is shown schematically in Fig.1. and consists of the main components which are further presented in the following sections.

2.1.1. Magnet cryostat

The cryostat is an enclosure made of non-magnetic stainless steel, with double vacuumed walls, designed to use and maintain liquid nitrogen at a low evaporation rate. Liquid nitrogen is used to cool the cryoelectromagnet at its boiling temperature (77K). At the same time, the cryostat also has the role of mechanically supporting the cryomagnet assembly.

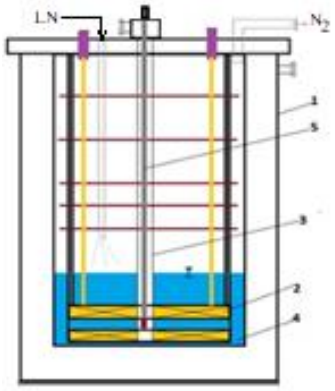

Fig. 1. Conceptual model of 5T pulsed cryomagnet
1-Cryostat; 2-Coils; 3- Central channel; 4-Liquid Nitrogen bath;5- Hall probe

2.1.2. The cryomagnet

Its role is to generate a short-lived pulsating magnetic field, which has two important characteristics: high uniformity (~ 0.1%) and high field value (~ 5T). The chosen construction solution consists of a Helmholtz system of conventional coils (copper conductor). The magnetic field is generated in the central channel of the electromagnet, in the space between the coils. Fig.2 shows schematically the pair of Helmholtz coils, where Di - is the inner diameter of the coils, De- is the outer diameter and d – is the distance between coils.

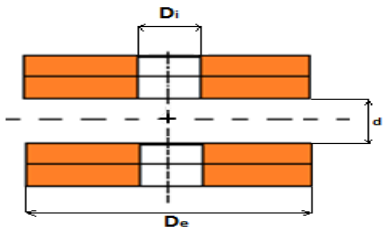

Fig.2. Helmholtz coil assembly - cross section.

Helmholtz coils are circular, designed to be made of 6 mm wide and 0.4 mm thick strip-type copper conductor. The coils will be cooled to 77K by immersion in liquid nitrogen, so that the resistivity of copper will decrease approximately 8 times compared to the resistivity of copper at room temperature (300K) [16].

2.1.3. The central channel

It consists of a stainless steel tube, which will be vacuumed and will allow access from outside the system to the area of the magnetic field generated by the

Helmholtz coil system. The vacuum level will be 10^{-3}-10^{-6} mbar, to avoid condensation in the channel.

2.1.4. Liquid nitrogen bath

Inside the cryostat, the liquid nitrogen introduced from a dewar, will create a "bath" of liquid nitrogen with a temperature of 77 K, so that the copper coils will be cooled to the same temperature. Once cooled, the coils can be subjected to a pulsating current to ensure the current necessary to obtain the magnetic field required by the application (0-5T).

2.2. Pulsed cryomagnet design

Fig. 2 shows the principle diagram of the electromagnet designed to generate a magnetic field with a maximum magnetic flux density of 5T in its center. The winding will be made of high purity copper conductor (99.99%) [21] in the form of a strip. The main characteristics of the electromagnet are presented in Table 1.

Table 1

The main features of the electromagnet

Characteristic	Value
Conductor width	6 mm
Conductor thickness	0.4 mm
Conductor thickness with insulation	0.52 mm
Inner diameter	30 mm
Outer diameter	290 mm
Central zone magnetic field*	5 T
Turns no. / single reel	250
Conductor length/ single reel	126 m
Conductor length /double reel	252 m
Electrical resistance of magnet at 295K	3.5586 Ω
Electrical resistance of the magnet at 77K	0.4396 Ω

*Maximal value

2.2.1. Magnetic flux density calculus

For the calculation of the magnetic field generated by the Helmholtz coil system, the data presented in Table 2 were used. The calculus was performed considering a stationary supply of the magnet with a constant current for the design of the magnet to generate a maximum 5T magnetic field density in the center of the system coils. But, the real operation of the magnet will be in nonstationary manner by supplying it with a rectangular shape pulse of the current.

Table 2

The main features of the Helmholtz coil system

Characteristic	Value
Conductor total length /one reel	125.6 m
Current	730 A
Current density	304.16 A/mm^2
Inner radius (Di)	15 mm
Outer radius (De)	145 mm
Conductor width	6 mm
Distance between coils (d)*	30 mm

*Shown in Fig.2.

The magnetic flux density in the center of the coil is calculated [22,23] with the relation:

$$B_z(0,0) = \mu_0 \cdot \lambda \cdot J \cdot a_1 \cdot F(\alpha \cdot \beta), \quad (1)$$

where $\mu_0=4\pi\times10^{-7}$ [H·m^{-1}] is the vacuum magnetic permeability, λ is a filling factor for the coils, J [A·m^{-2}] is the current density. *F(α, β)* is given by relation:

$$F(\alpha \cdot \beta) = \beta \cdot ln\left(\frac{\alpha+\sqrt{\alpha^2+\beta^2}}{1+\sqrt{1+\beta^2}}\right) \quad (2)$$

where α and β are geometric factors specific for a cylindrical coil and defined as:

$$\alpha = \frac{a_2}{a_1} \text{ and } \beta = \frac{b}{a_1}$$

For illustration of the significance for these parameters, see Fig.3.

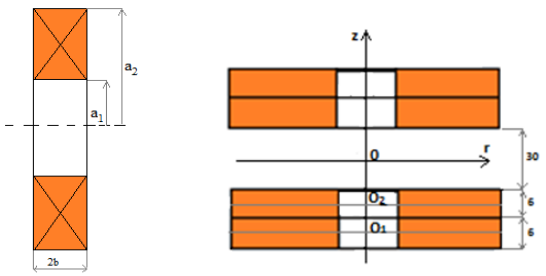

a. **b.**

Fig.3. Cylindrical coils, geometrical parameters.

Obviously, $D_i = 2\ a_1$ and $D_e = 2\ a_2$.

Considering the data from Table 2, results the values:

$$\propto = 9.66 \ \ and \ \ \beta = 0.2$$

Applying equations (1) and (2), results the value of the magnetic flux density in the center of a single coil (a single reel) (Table 3). To compute the magnetic flux density generated in center of a double coil (two wheel), we can use rel. (3).

$$B_z(0,0) = \mu_0 \cdot \lambda \cdot J \cdot a_1[F(\propto, 2 \cdot \beta)] \quad .(3)$$

The magnetic flux density at a certain distance z_1, towards the center of a coils system [23] is given by eq. (4):

$$B_z = \frac{1}{2}\mu_0 \cdot \lambda \cdot J \cdot a_1 \left\{ \left[\beta_1 \cdot ln \left(\frac{\propto + \sqrt{\propto^2 + {\beta_1}^2}}{1 + \sqrt{1 + {\beta_1}^2}} \right) \right] - \left[\beta_2 \cdot ln \left(\frac{\propto + \sqrt{\propto^2 + {\beta_2}^2}}{1 + \sqrt{1 + {\beta_2}^2}} \right) \right] \right\} \quad (4)$$

Where $\lambda = 0.77$ and β_1, β_2 are:

$$\beta_1 = \frac{b + z1}{a_1} \text{ and } \beta_2 = \frac{z1 - b}{a_1} \quad (5)$$

This equation will be used to compute the magnetic flux density in the center of the pair coils system. The results are summarized in Table 3.

Table 3

Summarize of the magnetic flux density calculations

Magnetic flux density	Eqs. involved	Value (T)
Center of a single coil	(1)+(2)	1.805
Center of a double coil	(3)	3.57
Center of the coils system	(4)+(5)	5.04

2.2.2. Electromagnet inductance calculus

The inductance for a single pancake coil [23], is obtained using the equation:

$$L \cong \mu_0 a_1 N^2 \left(\frac{\propto + 1}{2}\right) \left\{ ln \left[\frac{4(\propto + 1)}{\propto - 1} \right] \left[1 + \frac{1}{24} \frac{(\propto - 1)^2}{(\propto + 1)^2} \right] - \frac{1}{2} \left[1 - \frac{43}{144} \frac{(\propto - 1)^2}{(\propto + 1)^2} \right] \right\}. \quad (6)$$

Applying equation (6), results:

$$L \cong 16.396 \cdot 10^{-3} \text{ H}.$$

The total inductance of the two series connected coils is:

$$L_{12} = L_1 + L_2 + 2M_{12}, \tag{7}$$

where M_{12} is the mutual inductance of the coils. The coupling coefficient k is:

$$k = \frac{M_{12}}{\sqrt{L_1 L_2}}. \tag{8}$$

Using eq. (4), the magnetic flux density in the center of the system will be (see fig.3.b):

$$B_{total} = 2 \cdot [B_{24} + B_{18}] \tag{9}$$

Where B_{24} and B_{18} are the magnetic flux densities generated in the point O (center of the coils system), by the two pancake coils (with center O1 and O2).

For a double pancake coil, the distance between coils is approximately *0* and the coupling coefficient k = 1, thus obtaining for the mutual inductance M_{12} the value:

$$M_{12} = 16.396 \cdot 10^{-3} \text{ H}.$$

The total inductance of the double pancake coil is then

$$L_{12} = 65.58 \cdot 10^{-3} \text{ H}.$$

For long distances between two coils A and B mutual inductance $\boldsymbol{M_{AB}}$ can be calculated [22] with the equation:

$$M_{AB} \equiv \frac{1}{2}\mu_0 (N_A \cdot N_B)\sqrt{(a_A + a_B)^2 + g^2} \cdot \{2[K(k) - E(k) - k^2 K(k)]\} \tag{10}$$

where K(k) and E(k) are the complete elliptic integrals, respectively, of the first and second kind, defined as $K(k) = \int_0^{\pi/2} \frac{d\theta}{\sqrt{1-k^2 sin^2\theta}}$ and $E(k) = \int_0^{\pi/2} \sqrt{1 - k^2 sin^2\theta}\, d\theta$, $a_A = a_B = a_1$ are the inner radius of the coils and $N_A = N_B = 500$ are the turns number of each double pancake. Results

$$k^2 = \frac{4 a_A a_B}{(a_A + a_B)^2 + g^2} = 0.5 \tag{11}$$

and the factors $E(k) = 1.3506$ and $K(k) = 1.8540$.

Equation (10) will give: $M_{AB} = 3.24738 \cdot 10^{-3}$ H.

Thus, the inductance of the coils system which is given by:

$$L_{AB} = L_A + L_B + 2M_{AB}. \tag{12}$$

therefore: $L_{total} = 137.654 \cdot 10^{-3}$ H.

2.2.3. Magnetic energy stored in the coils system.

The total energy stored in the Helmholtz system given by:

$$W_{total} = \frac{1}{2}L_A {I_A}^2 + \frac{1}{2}L_B {I_B}^2 + \frac{1}{2}M_{AB}I_A I_B + \frac{1}{2}M_{BA}I_A I_B. \tag{13}$$

Using data obtained above, will result the total magnetic energy stored:

$$W_{total} = 36{,}677 \cdot 10^3 \text{ J}.$$

3. Numerical modeling of the cryomagnet

To find the maximum value of the magnetic flux density generated by a set of coils in a Helmholtz type arrangement, the Comsol Multiphysics software was used [24]. To find an optimal configuration for the dipole model to produce a magnetic field of 5 T intensity, 3 different cases were considered for modeling, in which the insulation size for the copper strip differs, namely: without insulation (thickness = 0.4 mm), with "type 1" insulation (thickness = 0.52 mm), with "type 2" insulation (thickness = 0.64 mm).

3.1. The mathematical model

The same model is used for all three cases mentioned above.

Due to the structure of the dipole, the magnetic field can be analyzed using an axi-symmetric model for numerical modeling. The stationary magnetic field is described by the following equation:

$$\nabla \times ({\mu_0}^{-1}{\mu_r}^{-1}\nabla \times \mathbf{A}) = \mathbf{J}_{\boldsymbol{\varphi}}^{\mathbf{e}}. \tag{14}$$

where **A** [T·m] is the magnetic potential vector (for this model, the angular component is the one used), $\mathbf{J}_{\varphi}^{e}$ [A·m^{-2}] is external current density, $\mu_0=4\pi\times10^{-7}$ [H·m^{-1}] is the vacuum magnetic permeability and μ_r is relative magnetic permeability, eq. (14).

The boundary conditions on the boundary of the geometric model are symmetry and magnetic insulation (**n** × **A** = 0, **n** being the out of plan normal).

3.2. The geometric model

Due to the geometric restrictions, the geometric model can be one for all the analyzed cases.

The domains representing the superconducting coils were set according to the data obtained through the analytic method presented in subchapter 2.2.1 of this paper. An air domain with the frontier condition of magnetic insulation, was chosed to enclose the coils. It size was set to be large enough so it does have a influence on the magnetic field generated by the superconducting coils.

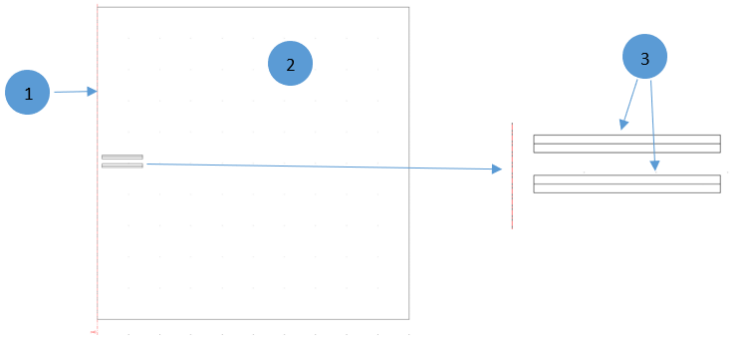

Fig.4. Geometric model - complete and detailed.

Fig. 4 shows the geometric model used in numerical modeling (1 - axis of symmetry, 2 - air domain, 3 – double reel coils).

3.3. Numerical modeling results

Only the case that, according to the numerical modeling, is optimal will be described. In this case, the following data were considered:

- I = 540 A;
- $L_{conductor/single\ reel}$ = 131 m;
- $L_{conductor/total}$ = 524 m;
- $N_{turns/single\ reel}$= 260;

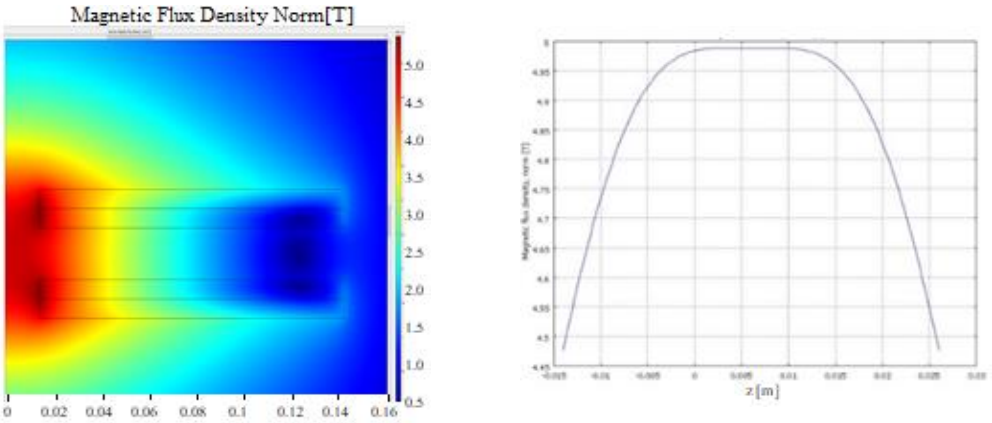

a) Magnetic flux density – color map b) Magnetic flux density – dipole centre

Fig.5. Magnetic flux density – color map and dipole centre.

Figure 5. a) is represented by the magnetic flux density in the form of a color map, the values are in Tesla. The maximum value of the magnetic flux density
is 5.39 T at the level of the superconducting coils.

Fig. 5. b) shows the variation of the magnetic flux density in the center of the dipole on the axis of symmetry. This reaches the desired value of 5 T.

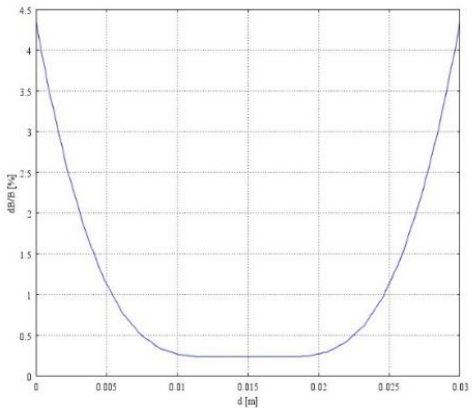

Fig.6. Non-uniformity of the magnetic field in the GFR area (good field area).

Table 4 shows the comparative analysis of the 3 cases considered in the modeling.

Table 4

Comparative analysis for 3 types of copper conductor

Case	I [A]	Turns No./bulk	Conductor thickness [mm]	B [T]	dB/B [%]
1	540	260	0.40	5	0.2
2	730	250	0.52	5	0.16
3	1100	204	0.64	5	0.4

4. Thermal analysis of the cryoconductive coil

4.1 The winding heating.

An analytical calculation was performed to determine the temperature that the coil will reach when it is fed. To reach the current of 700 A, a duration of approx. 1000 ms. This time required to load the coil was divided into four equal intervals of 250 ms each. The starting temperature is 77 K. Iterative calculations will be performed to determine the maximum temperature reached by the coil, knowing the properties of the material depending on the temperature at which it is.

Thus, the resistance of the coil will be given by well-known relationship:

$$R = \rho \frac{l}{S}. \tag{15}$$

Where:

- R – coil resistance [Ω];
- ρ – copper resistivity [Ω m];
- l – the conductor length [m];
- S – conductor section area [m^2].

Knowing the resistance of the coil, we can determine the power consumed by the coil:

$$P = R \cdot I^2. \tag{16}$$

where

- P – the power of the coil [W];
- I – the supply current of the coil [A].

The amount of heat released in a certain amount of time will be given by:

$$Q = P \cdot \Delta t. \tag{17}$$

where

- Q – generated heat [J];
- Δt – time interval [s].

Then, the temperature that the coil reaches for the considered time interval will be:

$$T_f - T_i = \frac{Q}{mC_p} \Rightarrow T_f = \frac{Q}{mC_p} + T_i. \quad (18)$$

where

- T_f – final temperature [K];
- T_i – initial temperature [K];
- m – mass [kg];
- C_p – specific heat [J/kg K].

Table 5 presents the results obtained, using values of electrical resistivity and specific heat of copper [16]. The value for the electrical conductivity was considered taking in account the temperature of the copper at the specified moment of time in Table 5. The temperature increases due the Joule heating that occurs in the conductor.

Table 5

Results from analytical calculations

t [s]	I [A]	T [K]	ρ [*10^{-8} Ω m]	C_p [J/kg K]
0.25	404	85.64	0.21	192
0.5	585	104.93	0.22	200
0.75	665	128.9	0.25	212
1	700	155.24	0.36	248
1.25	714	203	0.52	288

Thus, a calculation model was considered, which took into account the progressive heating of the winding as the current increased from 0 A to the final value of 700 A necessary to obtain a dipole magnetic field generated of maximum 5 T.

An increase in current within 1000 ms was considered. This time required to load the coil was divided into 4 subintervals of 250 ms each, for which the temperature rise of the coil was calculated. The modification of the parameters electrical resistivity and specific heat at the new temperature obtained were calculated each time and which were used in the calculation of the amount of heat released and of the temperature increase in the next time interval of 250 ms. The algorithm was repeated 4 times.

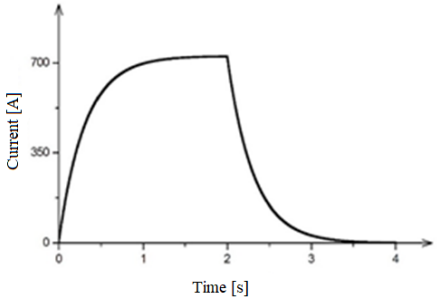

Fig.7. Typical electromagnet charging-discharging curve.

In Fig. 7 the typical charging-discharging curve of the pulsed electromagnet is presented, its charging current being 700 A, a duration for maintaining the current through the electromagnet coil of 1000 ms and a discharge interval of 1200 ms were taken into account.

In Fig. 8 the increase of the temperature in the copper cryoresistive coil is presented, for the time duration of 1000 ms necessary for its charging, up to the current value of 700A (data presented in Table 5).

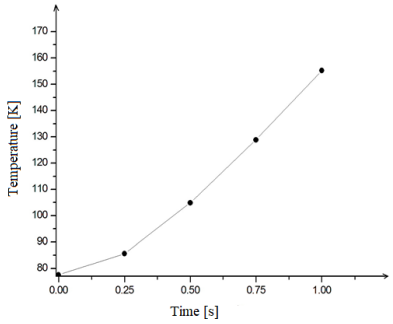

Fig.8. Temperature rise in the winding during a pulse.

4.2 Cryogenic cooling of the winding.

The amount of heat produced by the electromagnet due to the Joule effect during its supply with the current pulse, will be transferred entirely to the cooling liquid nitrogen bath in which the electromagnet is immersed. Thus, the liquid nitrogen bath will take over the heat produced in the winding. The liquid nitrogen has a temperature of 77 K (boiling temperature in normal conditions) and the heat transfer will contribute to direct evaporation of the liquid. The heat of vaporization for nitrogen being $q = 160.6 \left[\frac{J}{ml}\right]$ [21], the amount of liquid nitrogen consumed for a complete coil loading-unloading cycle can be computed. The results of the calculations are presented in Fig. 9 which shows the

consumption of liquid nitrogen (volume) depending on the heat produced during a complete cycle (several values of the generated heat are taken into account).

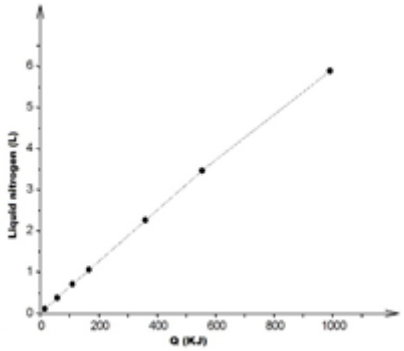

Fig.9. Consumption of liquid nitrogen, depending on the heat produced by the winding.

The maximum value was calculated for a current of 700 A and a total duration of the current pulse of 1 s (see table 5). A total amount of 6.23 l of liquid nitrogen/ coil will be evaporated.

5. Conclusions

The paper presented a conceptual model and design of a normal conductive electromagnet, cooled with liquid nitrogen, to obtain a dipole magnetic field of maximum 5T with high uniformity (0-3%). The main advantage of such an electromagnet is the relatively high value of the magnetic flux density of the generated magnetic field, for short time intervals. (~ 10^{-4} – 10^{-3} s), which does not generate excessive heating of the winding (ΔT ~130 K). Conceived in a constructive version of the Helmholtz type, the electromagnet has two double-row bucket-type sections, made of copper strip. The inner diameter of the winding is 30 mm, the outer diameter is 290 mm, and the distance between sections is 30 mm. The maximum magnetic flux density obtained as a result of numerical modelling with Comsol Multiphysics software, was 4.98 T for a maximum current of 730 A.

For each current pulse applied to the electromagnet, the amount of liquid nitrogen consumed by evaporation is ~ 7 l (for a cycle lasting 1 s).

Such an electromagnet is useful, especially in applied physics experiments, in which the presence of the magnetic field is not required continuously, for long periods of time, but only for short periods of time (~ ms), at good time intervals. defined. Such values of magnetic flux density (> 2T) cannot usually be obtained with conventional means (copper windings) but only with the

help of superconducting electromagnets which are generally much more expensive compared to conventional ones. The use of a cryogenic cooled electromagnet like the one proposed in the paper, allows overcoming technological limits and obtaining high values of magnetic flux density, but for short periods of time.

Acknowledgements

The authors would like to thank to Romanian Ministry of Research, Innovation and Digitization for financing the works through the Nucleu Program, under contract PN19310303 /2019.

R E F E R E N C E S

[1] A. B. - Holder, H. Keller," High-temperature superconductors: underlying physics and applications", Zeitschrift für Naturforschung B, Volume 75: Issue 1-2, DOI: https://doi.org/10.1515/znb-2019-0103, 2019.
[2] Fujikura Inc., https://www.fujikura.co.uk/products/energy-and-environment/2g-ybco-high-tempurature-superconductors/.
[3] A. Devred, Practical Low-Temperature Superconductors, https://cds.cern.ch/record/796105/files/CERN-2004-006.pdf.pdf, CERN, 2004.
[4] Furukawa Electric Co. https://www.furukawa.co.jp/en/rd/superconduct/smartgrid.html
[5] Bruker, https://www.bruker.com/products
[6] CERN, https://home.cern/news/opinion/physics/roadmap-future
[7] R. Zeng V. Murashov T. P. Beales H. K. Liu, S. X. Dou "High temperature superconducting magnetic levitation train", Applied Superconductivity, Volume 5, Issues 1–6, January–June 1997, Pages 201-204.
[8] W. V. Hassenzahl, "Applications of superconductivity to electric power systems," in IEEE Power Engineering Review, vol. 20, no. 5, pp. 4-7, May 2000, doi: 10.1109/39.841342.
[9] E. Darie and E. Darie, "Fault current limiters based on high temperature superconductors," 2007 8th International Conference on Electric Fuses and their Applications, Clermont-Ferrand, 2007, pp. 69-73, doi: 10.1109/ICEFA.2007.4419969.
[10] W.V. Hassenzohl, D. W. Hazelton, B.K. Johnson, Ch.T. Reis, "Electric Power Applications", Proceedings of the IEEE, Vol. 92, No.10, Oct. 2004.
[11] Joseph Minervini, Michael Parizh and Marco Schippers, "Design of a HTS cuadrupolar Magnet Focus on Superconducting Magnets for Hadron Radiotherapy and MRI" , Superconductor Science and Technology, Volume 31, Number 3, 2018
[12] A. M. Morega, I. Dobrin, M. Morega, A. Nedelcu and V. Stoica, "Design and numerical simulations of a superconducting dipolar electromagnet cooled by conduction," 2015 9th International Symposium on Advanced Topics in Electrical Engineering (ATEE), Bucharest, 2015, pp. 79-83, doi: 10.1109/ATEE.2015.7133680.
[13] I. Dobrin *et al*., "High Temperature Superconductor dipolar magnet for high magnetic field generation - design and fabrication elements," 2017 10th International Symposium on Advanced Topics in Electrical Engineering (ATEE), Bucharest, 2017, pp. 201-205, doi: 10.1109/ATEE.2017.7905109.

[14] I. Dobrin, A. M. Morega, A. Nedelcu, M. Morega and J. Neamtu, " A Conduction Cooled High Temperature Superconductor Quadrupolar Superferric Magnet, Design and Construction" Journal of Physics: Conference Series, Volume 507, Large Scale
[15] I. Dobrin, D. Enache, A. Dobrin, G. Dumitru, "Numerical modeling and design of a superconducting solenoid generator of 6T magnetic flux density", Scientific Bulletin of University Politehnica of Bucharest, 2020
[16] Sumitomo Cryogenics (SHI), http://www.shicryogenics.com
[17] Santosh Miryala, "Recent Superconducting Applications in the Medical Field", High Temperature Superconductors, ISBN 978-1-53613-341-7, Nova Science Publishers, Inc., 2018., Chapter 15.
[18] Kzysztof Malinowski, "Applications of superconductivity in medicine", https://indico.cern.ch/event/445524/contributions/1951038/attachments/1192904/1731951/Application_of_superconductors_in_medicine1.pdf.
[19] Sunpower Inc., http://www.sunpowerinc.com/
[20] Jack W. Ekin, "Experimental Techniques for Low-Temperature Measurements, Cryostat Design, Material Properties, and Superconductor Critical-Current Testing", Oxford University Press Inc. New York, 2006, ISBN 0–19–857054–6, 978–0–19–857054–7
[21] Luvata, https://www.luvata.com/products/ultra-pure-copper-products
[22] D. Bruce Montgomery, "Solenoid Magnet Design. The Magnetic and Mechanical Aspects of Resistive and Superconducting Systems", Interscience (Wiley), New York, 1969.
[23] Yukikazu Iwasa, Case Studies in Superconducting Magnets: Design and Operational Issues, ISBN-13: 978-0306448812, Springer, 2009.
[24] Comsol Multiphysics, https://www.comsol.com.